Coupled Systems Mechanics, *Vol. 3, No. 2 (2014) 195-211*
DOI: http://dx.doi.org/10.12989/csm.2014.3.2.195

Coupling of nonlinear models for steel-concrete interaction in structural RC joints

Norberto Domínguez* and Jesús Pérez-Mota[a]

Department of Postgraduate and Research Studies (SEPI) ESIA UZ National Polytechnic Institute of Mexico, Edificio de Posgrado e Investigación, Av. Miguel Bernard s/n 07300 Mexico D.F., Mexico

(Received March 25, 2014, Revised June 2, 2014, Accepted June 3, 2014)

Abstract. When strong seismic forces act on reinforced concrete structures, their beam-column connections are very susceptible to damage during the earthquake event. The aim of this numerical work is to evaluate the influence of the internal steel reinforcement array on the nonlinear response of a RC beam-column connection when it is subjected to strong cyclic loading –as a seismic load. For this, two specimens (extracted from an experimental test of 12 RC beam-column connections reported in literature) were modeled in the Finite Element code FEAP considering different stirrup's arrays. In order to evaluate the nonlinear response of the RC beam-column connection, the 2D model takes into account the nonlinear thermodynamic behavior of each component: for concrete, a damage model is used; for steel reinforcement, it is adopted a classical plasticity model; in the case of the steel-concrete bonding, this one is considered perfect without degradation. At the end, we show a comparison between the experimental test's responses and the numerical results, which includes the distribution of shear stresses and damage inside the concrete core of the beam-column connection; in the other hand, the effects on the connection of a low and high state of confinement are analyzed for all cases.

Keywords: beam-column connection; reinforced concrete; non-linear material behavior; finite element

1. Introduction

In civil engineering construction, one of the most important hybrid materials used widely is the Reinforced Concrete (RC), and its efficiency depends on different aspects related not only to structural design but also to constructive techniques. In both cases, the accomplishment of the local regulatory requirements should guarantee the structural safety of RC structures (in other words, design rules and construction codes, as reviewed by Sasmal and Ramanjaneyulu (2012)): unfortunately, due to the complexity of RC, these requirements adopt many technical simplifications in order to reduce the effects of uncertainties. In the case of structural design of RC buildings, the required level of security ought to be reached by specifying the geometrical dimensions of each structural element that compounds the system (columns, beams, walls, slabs … and their joints) as well as the quantification and location of the respective internal steel reinforcement. The specific behavior of each structural element has been widely studied even for

*Corresponding author, Professor, E-mail: ndominguez@ipn.mx
[a] Post-graduate student, E-mail: ikse150480@hotmail.com

http://www.techno-press.org/?journal=csm&subpage=7 ISSN: 2234-2184 (Print), 2234-2192 (Online)

thermal effects (Ngo *et al.* 2014) and their respective results have served to create a large set of constructive/design specifications, in order to assure that the structural element will develop the expected loading capacity. Nevertheless, this capacity does not rely only on a good transference of internal forces and stresses between concrete and steel bars, but also on the boundary conditions of the structural element, which are defined physically by the joints that connect these structural elements. Due to its importance, it is necessary to improve the mechanical knowledge of RC joints as well as avoiding any damage on them (a good description of the distribution of internal forces inside a joint is done by Zhou and Zhang (2012)). Some researchers have focused in improving the structural response of the joint through the use of anchor-type intermediate bars and advanced details of doubly confined closed stirrups in the beam near the joint (Ha and Cho 2008).In spite of this, it is very common that a blind application of these design specifications complicates unnecessarily the construction layout of the structural elements, in particular the layout of the beam-column connections, which are at the same time, the key-points for the structural stability of the whole system. In the other hand, to remove any steel rebar in an unreasoned way might reduce dramatically the resistance of the joint, particularly in the event of an earthquake, and this situation might drive to search new –and expensive- ways of rehabilitation/reparation (Wang 2012, Karayannis and Sirkelis 2008, Ha *et al.* 2012). Being the beam-column connection the main point of transmission of forces between horizontal elements (beams) and vertical elements (columns), it should provide enough stiffness to the global structural system. Consequently, there is a high concentration of stresses inside the connection, which potentially might produce damage in concrete and/or plastic deformations on steel bars. Some recent experimental works have focused in determine which parameters can affect the shear resistance of this kind of joints (Kim and LaFave 2007, Wong and Kuang 2011). That is the reason why beam-column connection is one of the most risky points of failure in RC structures.

On the other hand, the modern design is becoming strongly dependent of the numerical method adopted for structural analysis –commonly a standard finite element code- and the prediction of the realistic response (forces and displacements) is directly derived from the computational capabilities of the selected software. A non-initiated engineer in numerical simulations may believe that modeling of any mechanical problem concerns only the definition of a set of load combinations, forgetting that a numerical model should include as well: the choice of a proper finite element, the association to an efficient material model, and a good representation of the real boundary conditions. Paradoxically, even if the computational resources becomes powerful and user-friendly, the local study of any RC connection is practically disregarded by structural engineers -maybe for the complexity of preparing a full detailed modeling-, while steel reinforcement array is basically proposed from practical recommendations extracted from limited experimental tests. In consequence, the quantity of steel reinforcement inside the connection might be overestimated or simply poor distributed. According to Alcocer (1991), the Beam-Column (B-C) connections can be classified following two criteria:

- By the geometrical configuration of the steel reinforcement,
- By the local behavior of the full connection.

Accordingly to the first criterion, there are B-C connections with internal joints -when the beam's steel bars pass across the joint (see Fig. 1(a)) - and B-C connections with external joints -when the beam's steel bars are anchored inside the joint (see Fig. 1(b)). Based on the second criterion, there are elastic B-C connections (that means, any plastic behavior occurs out of the joint) and inelastic B-C connections (if any nonlinear phenomenon appears into the joint).

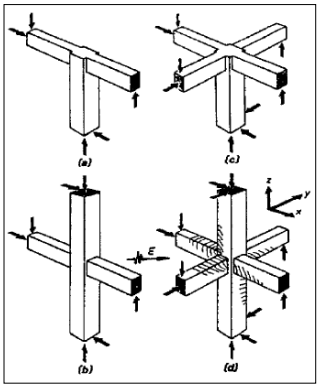

(a) Internal joint

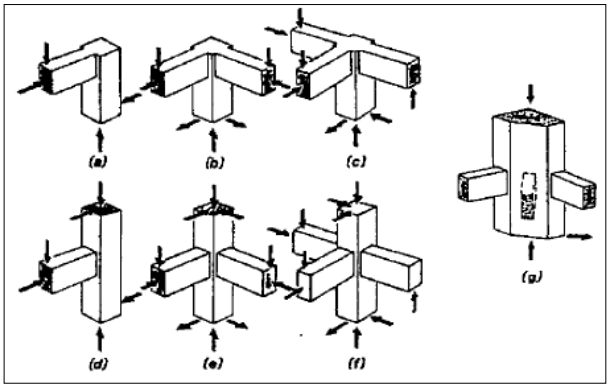

(b) External joint

Fig. 1 Classification of beam-column connections according to Alcocer(1991)

In conventional structures, the beam-column connection must be designed not only against the development of any nonlinear phenomenon inside, but also it should induce the failure out of the connection. The most accepted criteria of failure for the connected members is the SC-WB (Strong Column – Weak Beam), which means that if any plastic articulation is developed in the structural system, it should appear on the beam instead of on the column (Visintin *et al.* 2012). In spite of these recommendations, the B-C connection might fail, and the most common mechanisms of failure identified by different authors (Ma *et al.* 1976, Meinheit and Jirsa 1977, Lowes and Moehle 1995, Lowes 1999, Lowes *et al.* 2004) are the following:

- Beam reinforcement anchorage is not enough inside the joint and the bar slips,
- Shear forces developed into the joint activate the inelastic response of the core of concrete.
- A poor transference of shear forces may produce a failure plane between the joint and the beam, or between the joint and the column.

Based on numerical simulations, the aim of this work is to study how the quantity and distribution of the steel reinforcement array inside the RC beam-column connection affects its structural response when a strong cyclic loading is applied. For this, different stirrup's arrays and quantities are considered into the model. In these simulations, the nonlinear response of the RC beam-column connection is evaluated taking into account the nonlinear thermodynamic behavior of each component. For concrete, it was adopted a damage model proposed by Mazars (1986); for steel reinforcement, a classical plasticity model with Von Mises criterion was used; in all of the cases, the steel-concrete bonding was considered perfect –that means, without any degradation. In order to build a realistic model, the experimental results of a RC beam-column connection reported by Alamedinne and Ehsani (1991) are taken as reference. The numerical simulations were carried out in the Finite Element code FEAP (Taylor 2005), in which the concrete damage model was implemented adapting a user material subroutine.

2. Basis of the non linear modeling

2.1 The experimental test of reference

For the numerical study, the experimental work carried out by Alameddine and Ehsani (1991), was taken as a reference. It consisted in obtaining the structural response of an external beam-column joint subjected to cyclic loading, in order to verify the recommendations of the ACI-ASCE-352 code. The researchers classified the tests in three sets of four specimens, each set with a specific concrete high resistance. In all of the tests, three variables were observed and studied:

a) The compressive strength of concrete was 55.8 MPa (8 ksi), 73.8 MPa(11 ksi) and 93.8 MPa (14ksi) respectively;
b) The maximal value of the shear stress into the connection, with a minimal value of 7.6 MPa (1100 psi) and a maximum of 9.7 MPa (1400 psi); and
c) The contribution of the stirrups by improving the confinement of the core of concrete (see Table 1 for stirrup characteristics).

Each specimen was designated by two letters and a number, indicating: the level of the maximal joint shear stress (first letter), the level of confinement induced by the number of stirrups (second letter) and the value of the compressive strength. For example, the LH11 denomination designates a specimen with a "*Low*" shear stress (L), "*High*" confinement level (H), and a compressive strength of 11 ksi (11).

Table 1 Reinforcement on the transversal section of specimen's elements

Specimen	LL	LH	HL	HH
A_{s1c}	2 # 8, 1 # 7	2 # 8, 1 # 7	3 # 8	3 # 8
A_{s2c}	2 # 7	2 # 7	2 # 8	2 # 8
A_{s3c}	2 # 8, 1 # 7	2 # 8, 1 # 7	3 # 8	3 # 8
A_{s1b}	4 # 8	4 # 8	4 # 9	4 # 9
A_{s2b}	4 # 8	4 # 8	4 # 9	4 # 9
Number of stirrups	4	6	4	6
r_t	1.2	1.8	1.2	1.8
$h_s/d_{b,col}$	20	20	20	20
Development length l_{dh}(inches) required for $f'c$=8,000 (psi) (Recommendations 1985)	8.9	8.9	10.0	10.0
Development length l_{dh} (inches)	10.5	10.5	10.5	10.5

Notes:
1 psi = 6.89 kPa; 1 inch = 25.4 mm; L: Low; H: High; the first letter indicates the level of shear stress; the second letter indicates the level of confinement.

Fig. 2(a) shows the geometrical characteristics of the specimen. Applying a cyclic controlled displacement test (see Fig. 2(b)), the initial displacement in the free edge of the beam was of ± ½ inches (13 mm), being increased in ± ½ inches (13 mm) in each cycle of loading. During the test, a

small axial load was applied in the top of the column. At the end of the test, they reached distortions up to 7% corresponding to a maximum displacement of 4 ½ inches (114 mm), concluding that:

- Elevated shear stresses reduce significantly the load capacity of the connection.
- The value of the ultimate shear stress recommended by the ACI-ASCE-352 for the joint was lower than the value observed in the experimental tests for high resistance concrete.
- The increment of transversal reinforcement reduces the deterioration into the connection, avoiding the failure of the reinforcement anchorage.

Concerning to the expected ultimate loading capacity of each RC beam-column connection, it is assumed that this condition occurs when tension stress in the steel reinforcement reaches a value 25% higher than the nominal yield stress of the reinforcing steel. Specimens with a low shear level and high joint confinement were able to develop the ultimate capacities in the beams with a variation of ± 3.8% from the predicted capacities. In addition, these same specimens had the least stiffness degradation and loss of load-carrying capacity at displacement beyond the yield displacement.

2.2 Description of the thermodynamic nonlinear models adopted for numerical simulations

Because the main objective of this research is to evaluate the influence of the reinforcement into the structural response of a B-C connection, it is necessary that numerical simulations rely in a set of robust nonlinear models that reproduce the realistic behavior of each concerned material. In order to accomplish with this challenge, for each material some respected nonlinear models based on a thermodynamic formulation were adopted (a damage model for concrete; a classical plasticity model for steel)and combined afterwards into the model, in order to include the effects of the different dissipative phenomena associated to each inelastic material behavior.

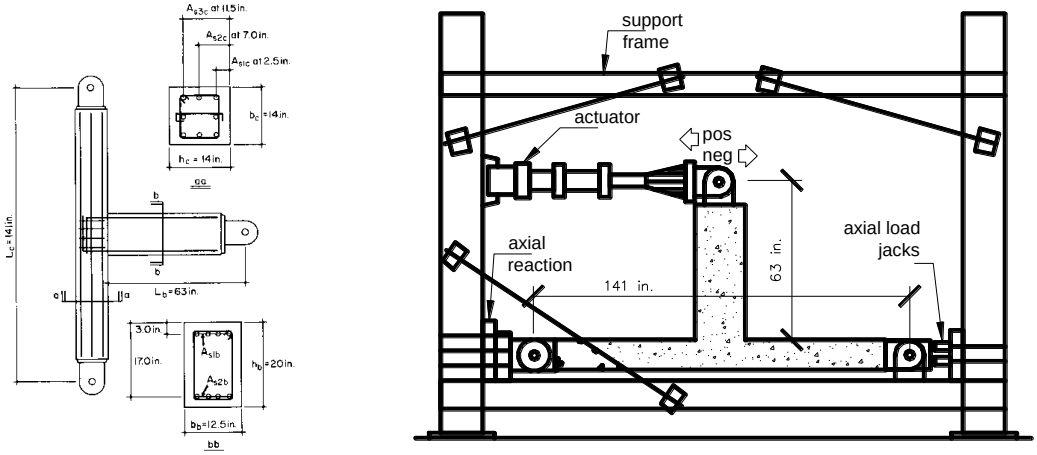

(a) Dimensions of the specimen in inches (b) Mounting of the experimental test

Fig. 2 Description of the experimental test according to Alameddine and Ehsani (1991)

2.2.1 Concrete behavior: the nonlinear damage model of Mazars

Due to the non-symmetric behavior of concrete, Mazars (1986) conceived a specific model in which the compression's damage is different compared to tension's damage. As any other similar model of damage, this one is formulated in order to represent the loss of continuity when multiple cracks appear and grow inside the concrete. In other words, the damage in a Representative Elementary Volume (REV) corresponds to a superficial density of micro-defects that can be expressed by the Eq. (1)

$$D = \frac{S_D}{S} \tag{1}$$

In which S is a transversal surface without any damage, S_D is the effective surface of transfer of stresses and forces, and D is the relationship between both surfaces, and in other words, the scalar variable of damage which goes from a value of zero (undamaged material) to one (full damage).

In a general damage model, the calculation of an effective stress is done by affecting the elastic modulus of the concrete E by a variable of damage (see Eq. (2), in which ε^e is the elastic strain). In the particular case of the damage model proposed by Mazars, this damage variable is replaced by two scalar damage variables, D_c and D_t - tension and compression damage respectively- (Eqs. (3) and (4)) that are activated as soon as a limit elastic strain is reached. Nevertheless, instead of building the surface of failure in the space of stresses, this one is built in the space of strains, needing the calculation of an equivalent strain (Eq. (5)).

$$\sigma = (1-D)E : \varepsilon^e \tag{2}$$

$$D = \alpha_t D_t + \alpha_c D_c \tag{3}$$

$$D_i(\tilde{\varepsilon}) = 1 - \frac{(1-A_i)\varepsilon_{d0}}{\tilde{\varepsilon}} - \frac{A_i}{\exp[B_i(\tilde{\varepsilon} - \varepsilon_{d0})]} \qquad (i = t, c) \qquad only \qquad if \qquad \tilde{\varepsilon} > \varepsilon_{d0} \tag{4}$$

$$\tilde{\varepsilon} = \sqrt{\sum_i \left(\varepsilon_i^+\right)^2} \qquad \varepsilon_i^+ = \max(0, \varepsilon_i) \tag{5}$$

In the last equations, ε_{d0} corresponds to the elastic tension strain limit that controls the beginning of damage for tension or compression; $\alpha_t, \alpha_c, A_i, B_i$ are model parameters that can be determined from experimental tests; the values adopted in this research are presented in Table 2, and the stress-strain relationship derived of the model is shown in Fig. 3. For the case of a cyclic loading, the damage model is able to take into account the cracks closure, avoiding any permanent deformation as it occurs in a plastic model: the unloading branch goes directly to zero deformation even for tension or compression loading in the corresponding stress-strain curve.

Table 2Material parameters for concrete using the damage model of Mazars

E (MPa)	32778	ε_{do}	7.428E-05
υ	0.16-0.2	A_c	1.446
f'c (MPa)	55.85	B_c	1570
Confinement index	1.06	A_t	0.97
ft (MPa)	2.8	B_t	8000

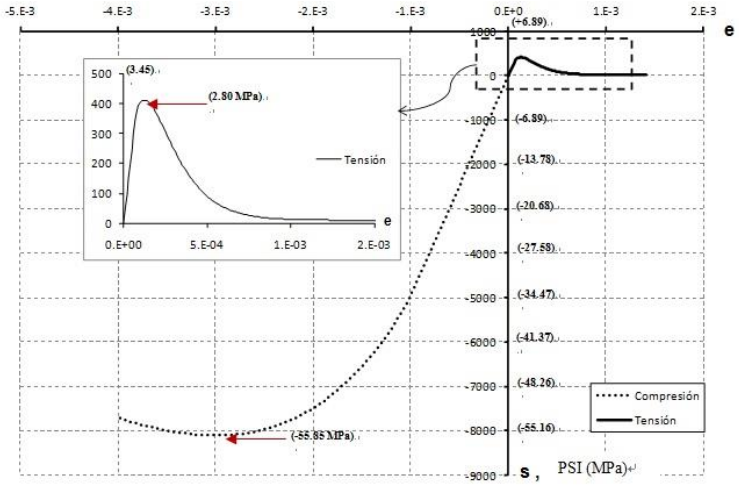

Fig. 3 Stress-strain curve for concrete behavior based on the damage model of Mazars

2.2.2 Steel behavior: a classical nonlinear plasticity model with hardening

For the reinforcing steel bars was chosen a classical elasto-plastic model based on Von Mises Criterion. It includes isotropic hardening. According to this criterion, plasticity does not start while (see Eq. (6))

$$\sigma_{eq} \leq \sigma_y \tag{6}$$

Being σ_{eq} the equivalent stress of Von Mises, calculated with the expression (Eq. (7))

$$\sigma_{eq} = \sqrt{\tfrac{1}{2}\left[(\sigma_1 - \sigma_2)^2 + (\sigma_2 - \sigma_3)^2 + (\sigma_3 - \sigma_1)^2\right]} \tag{7}$$

Based on Eq. (7), Fig. 4 shows the classical plastic yield surface based on Von Mises Criterion:

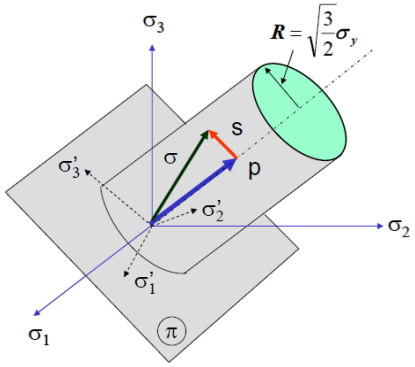

Fig. 4Yield surface for steel elastic-plastic behavior based on the Von Mises Criterion

Table 3 Material parameters for the elasto-plastic model adopted for the steel rebars

E (MPa)	199958
υ	0.3
fy (MPa)	248.11
$H_{isotropic}$(MPa)	60000

For a detailed description of classical plasticity models, it is recommended to consult specialized bibliography (Chakrabarty 2006, Ibrahimbegovic *et al*. 1998, Ibrahimbegovic 2009).

The parameter values adopted for the steel reinforcement are shown in the Table 3.

3. Numerical analysis of the beam-column connection

3.1 Description of the numerical strategy adopted for the analysis of the B-C connection

The numerical simulations of the Beam-Column connection were carried out in the finite element code FEAP v.7.4 (Taylor 2005), an open-source code with license in which is possible to implement user material models and user finite elements. For this research, the 3D damage model of Mazars was specifically implemented into the code, but due to the limitations of computational memory capacity, the beam-column connection was finally modeled in a 2D-space, which it is able to provide acceptable results –in comparison with 3D models- if some simplifications are done. For example, in a real RC structural element, the steel reinforcement forms a cage embedded into the concrete, inducing a particular concentration of stresses in the concrete around each bar. However, taking into account that bending is acting only in one plane, and assuming that the most important shear stresses might be developed in the same plane, it is possible to "homogenize" the steel reinforcement in layers for a 2D simulation. In the case of the stirrups, only the branches parallel to the bending plane are taken into account, modeled with one truss element whose transversal section corresponds to the total area of the stirrups. Because the concrete cannot develop large rotations, any possible geometrical non-linearity was not considered into the model.

The strategy followed in this research is described in the next steps:

a) Selection of the experimental reference
b) Definition of the cases to simulate:
   - only longitudinal steel without stirrups;
   - with minimal quantity of stirrups;
   - with the quantity of stirrups indicated in experimental test,
c) Comparison of results

3.2 Construction of the numerical model

Based onto the proposed strategy described before, the LL11 and LH11 specimens were

selected among the 12 corner-reinforced concrete beam-column subassemblies reported in the experimental reference, having both of them the same geometrical and material properties, except for the number of stirrups inside the core of concrete (four stirrups for "Low confinement", and six stirrups for "High confinement").

The basic model was constructed in a 2D space based on a plane strain formulation, using QUAD4 elements (4-node quadrangular element with 4 integration points) for the concrete body and TRUSS2 elements (2-node bar element) for the steel reinforcement. Initially, the reinforcement was modeled using QUAD4 elements as well, but due to their minimal dimensions, there were some numerical problems by a non-realistic excessive concentration of stresses around the union between longitudinal steel and the stirrups. Concerning to the bonding, it was modeled as perfect: in other words, the steel bar nodes are directly linked to the concrete body nodes. About boundary conditions, the bottom face of the column is fully-restrained, while the top face of the column was constrained only in the transversal direction because a constant axial load was applied and distributed at the same face. Moreover, the free edge of the beam is restrained in the axial direction, with a cyclic displacement imposed in its transversal direction (see Fig. 5(a)).

In the experimental test, at least eight displacement transducers were positioned in each Beam-Column connection in order to follow the evolution of displacements over the concrete face of the joint (see Fig. 5(b)). In the same way, we followed the numerical evolution of these points, in order to construct the corresponding load-displacement response.

In order to include the confinement effect induced by the stirrups and longitudinal reinforcement to the internal concrete, the model simulates two kind of concrete behavior, defining two regions delimited by the longitudinal bars: "internal confined concrete" and "unconfined external concrete" (see both regions on a section of the model in Fig. 6).

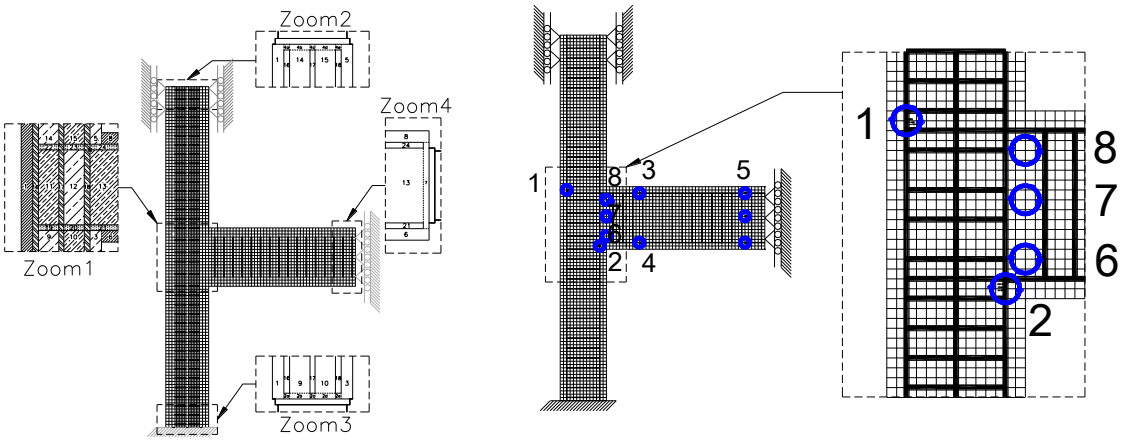

(a) Boundary conditions and reinforcement array

(b) Observation points of the stress-strain relationship according to the experimental tests

Fig. 5 Meshing details of the beam-column connection

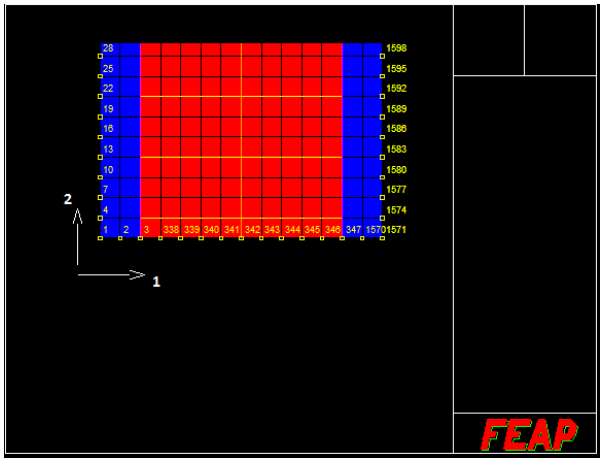

Fig. 6 Definition of the two concrete materials included into the model: Confined (in red) and unconfined (in blue) region

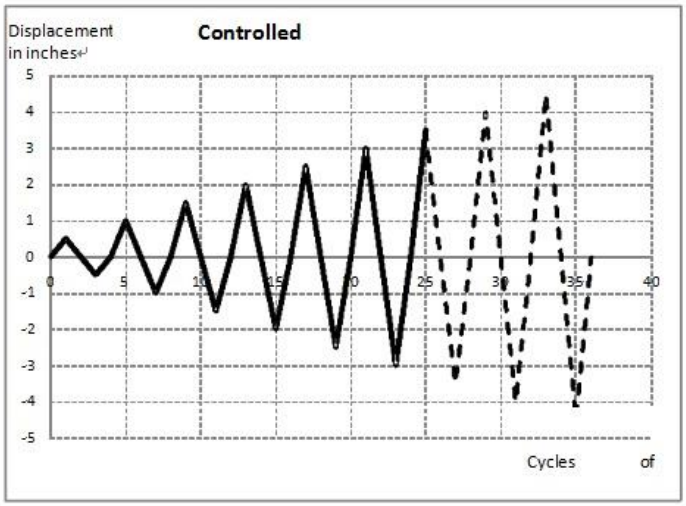

Fig. 7 Controlled displacements applied on the numerical simulations

Concerning to the cycling loading, it was applied a cyclic controlled displacement with an initial value of ± ½ inches (13 mm), being increased in ± ½ inches (13 mm) in each cycle of loading, as it is shown in Fig. 7. However, in contrast to the experimental tests in which the specimens were subjected to nine cycles of loading, in the simulations only six cycles of loading were analyzed due to problems of convergence, associated to the total damage of concrete in some finite elements.

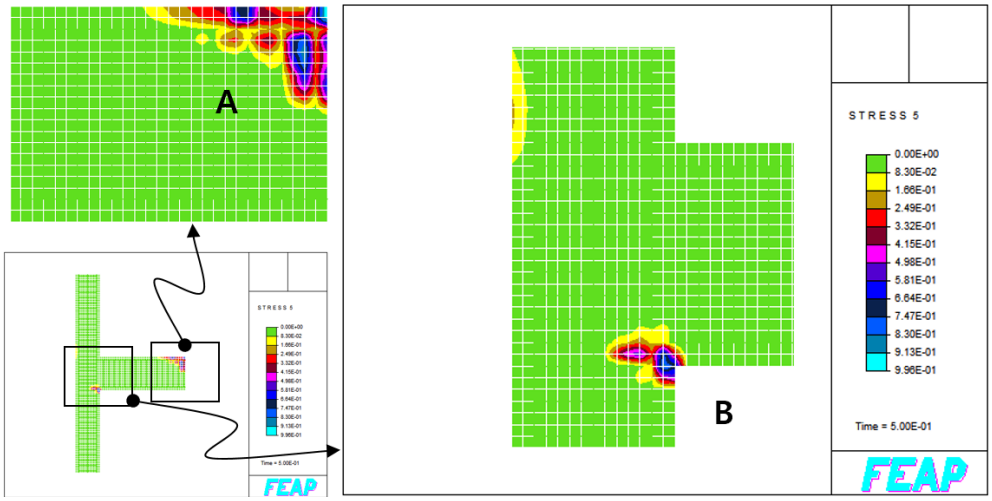

Fig. 8 Initial damage in the RC connection during the first cycle of loading: Premature damage in region A, and expected damage in region B

4. Discussion of the results

By comparison with the experimental results, we will discuss the numerical results obtained in the simulations, in which we provided a coupling of the nonlinear behavior of steel and concrete. Here it is important to mention that in experimental models, beam and column elements were over-reinforced in order to concentrate the damage only inside the joint. Unfortunately, in the numerical simulations is very difficult to avoid that damage appears immediately in some specific elements of the beam, out of the joint and near of the boundaries, as it is shown in Fig. 8. In this figure, letter A indicates the region with a premature damage near to the boundaries of the beam; letter B indicates the region with expected damage observed in experimental tests. This problem was solved by modifying some of the tension damage parameters in the affected finite elements, in particular the parameter ε_{d0} that controls the elastic strain limit, increasing its value until 10 times, delaying the damage in this zone.

Once solved the inconvenient, the discussion of results should focus in the comparison of the structural response of the two specimens, both experimental and numerical. Figs. 9(a)-9(c) correspond to the LL11 specimen, in which the maximal load capacity was reached between 40 and 45 kips for a displacement near to two inches. For the LH11 specimen, Figs. 9(b)-9(d) show a maximal load capacity near to 60 kips, very close to three inches of displacement. By comparing experimental curves with numerical results, it can be appreciated that some key-values are very similar (maximal load capacity associated to the lateral displacement), but the shape of their dissipative hysteresis loops are far away from any similitude. In numerical curves, all the unloading branches go directly to the origin, without any accumulated permanent displacement as it is observed in the experiments. Typically, the origin of these permanent displacements is associated to the crack friction on concrete. For cyclic loads, the damage model of Mazars includes only the slope variation of the elastic unloading, since cracks on concrete close as soon as there is

a reversibility of loading, assuming no friction on cracks. Because of this, it is not possible to reproduce numerically any dissipative loop or permanent deformation. This was already explained by Ragueneau *et al.* (2000), who presented a modified version of Mazars model which includes these effects. One possibility to deal with this problematic is to introduce a plastic formulation coupled to the damage model as it is proposed by Markovic *et al.* (2006), who present a coupled volume approach where the REV is linked with a fine-scale cell using a multi-scale strategy. In the same line, another strategy is to adopt the visco-elastic-plastic-damage model proposed by Jehel *et al*. (2012) which is able to take into account the seismic effects on the local degradation of concrete.

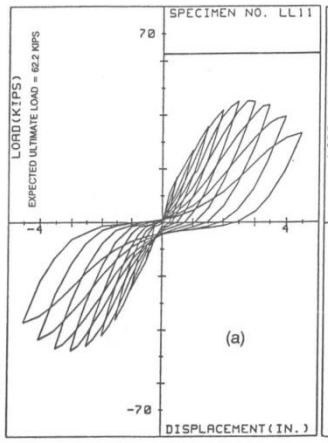

(a) Experimental curve for specimen LL11 adapted from Alamedinne and Ehsani (1991)

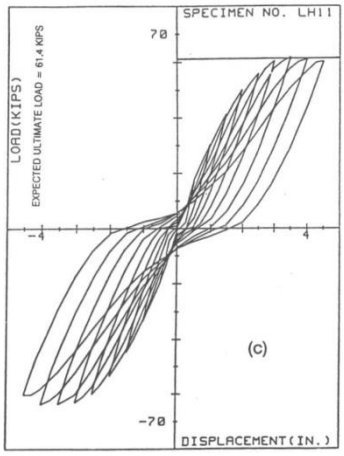

(b) Experimental curve for specimen LH11 adapted from Alamedinne and Ehsani (1991)

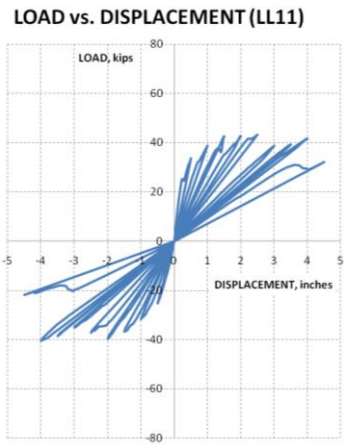

(c) Numerical curve for specimen LL11

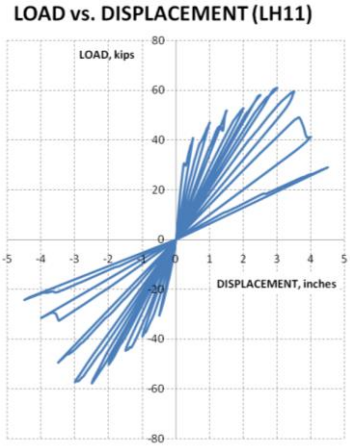

(d) Numerical curve for specimen LH11

Fig. 9 Load-displacement structural response of the beam-column connection

The second item of discussion is the distribution of principal and shear stresses inside the specimens, as it is shown in Figs. 10-12. As appreciated in Fig. 10, principal stresses reach their maximal value along the longitudinal steel rebars, which explains the premature damage on the neighbor concrete elements, as it was discussed previously for Fig. 8. In Figs. 11-12, the concentration of shear stresses is determined by the disposition of the stirrups, being greater the affected area when the reinforcement is lower inside the core. In fact, when no stirrups are placed inside the core, the damage is reached almost immediately, even if the longitudinal bars of the column and beams pass through the joint. Other relevant points observed in numerical simulations are the following:

a) In both cases, the maximum value of shear stress was reached on the beam, and not in the column or in the connection;

b) When the number of stirrups is increased inside the core, the principal damage is placed out of the core, exactly in the plane of connectivity between the beam and the core of the connection (as it is observed in Fig. 12); and

c) If the constant axial load on the column is not included into the model, the resistance of the beam-column connection decreases substantially, which agrees with Park and Paulay (1997).

d) The nonlinear behavior of the steel reinforcement was never activated in none of the simulations.

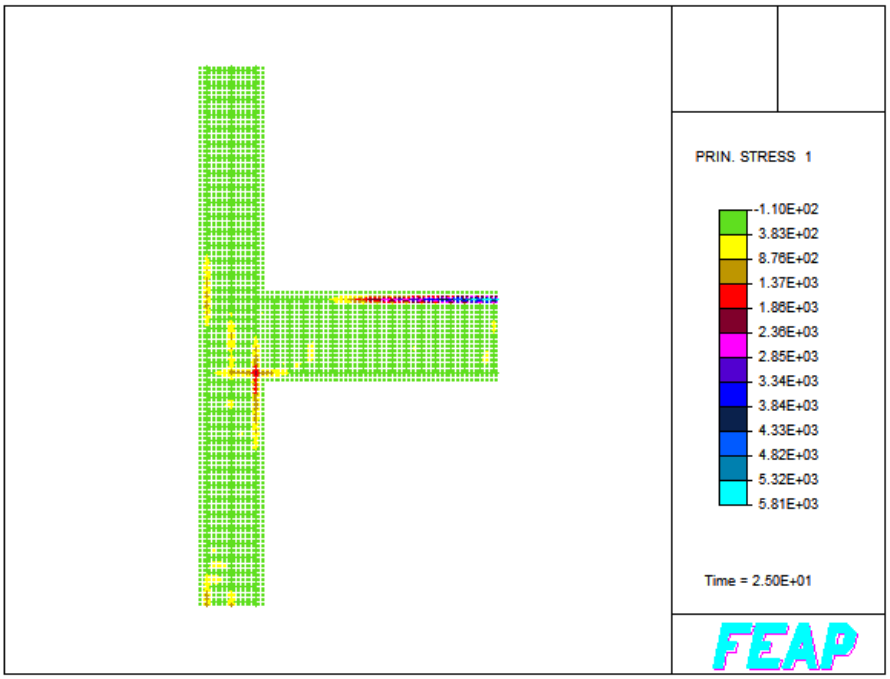

Fig. 10 Principal stress distribution on specimen LL11 (**LOW**confinement) for a displacement of 3.5 inches

In general, all the numerical simulations stopped as soon as a non-convergence condition was reached. Sometimes this problem was solved by reducing the time step, in particular in the picks of the displacement when unloading started. From a physical point of view, this non-convergence corresponds to the instant when a set of concrete elements reaches a high level of damage. It is interesting to compare this numerical condition with a comment of the experimental researchers (Alamedinne *et al*.1991), who mentioned in their work that the applied loading was very severe, in particular the final cycles of loading which are very unlikely to be experience by any real structure. In Figs.11-12, the level and distribution of damage in concrete can be observed for both specimens respectively. Apparently, damage is larger in LH11 specimen, but in fact, its response is more efficient than LL11 specimen's response, because the damage is better distributed along the stirrups, although the numerical value seems to be elevated. The implementation of bond elements must reduce this effect on the concrete body, as it was demonstrated by Dominguez *et al*. (2005), due to the redistribution of stresses induced by bonding, which allows a small slip or a small decohesion between steel bars and concrete, avoiding a false premature degradation of concrete as it is observed in these simulations.

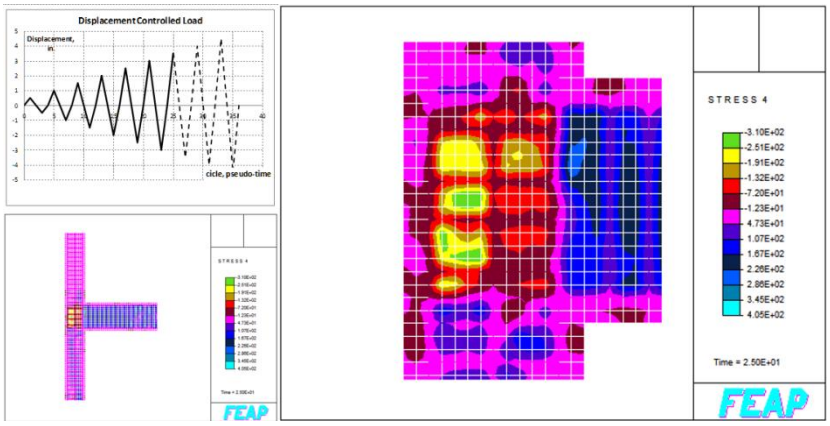

Fig. 11 Shear stress distribution on specimen LL11 (**LOW** confinement) for a displacement of 3.5 inches

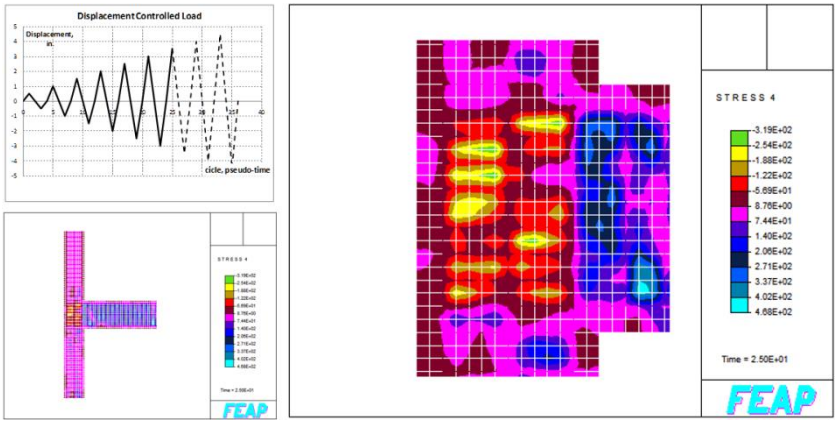

Fig. 12 Shear stress distribution on specimen LH11 (HIGH confinement) for a displacement of 3.5 inches

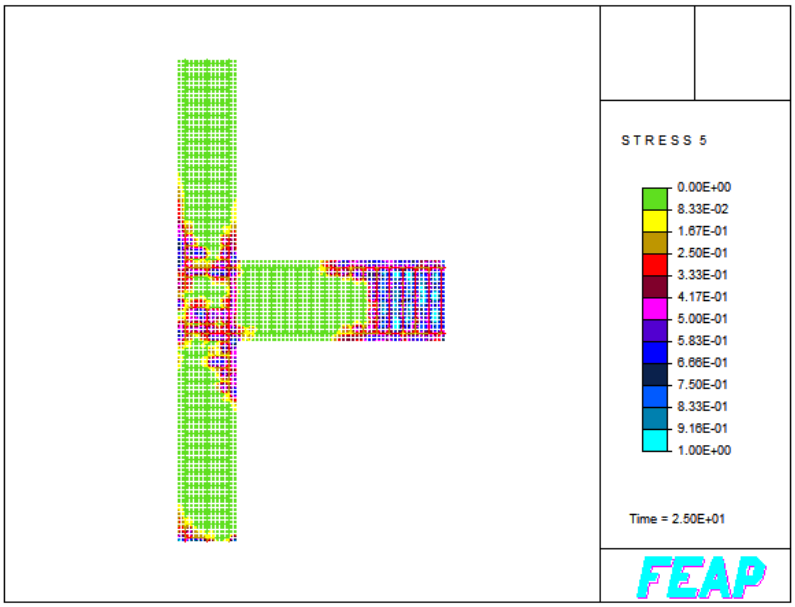

Fig. 13 Damage distribution on specimen LL11 (LOW confinement) for a displacement of 3.5 inches

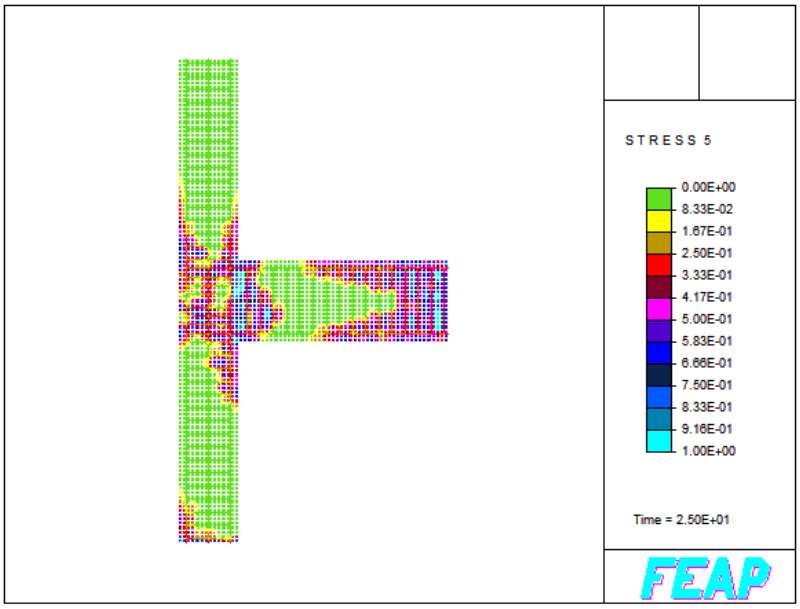

Fig. 14 Damage distribution on specimen LH11 (**HIGH** confinement) for a displacement of 3.5 inches

5. Conclusions

This work focused in studying the effect of the quantity and array of the shear steel reinforcement on the structural response of a RC beam-column connection, when it is subjected to cyclic loading. The simulations were performed combining two different thermodynamics nonlinear material models: a damage model for concrete, and a classical plasticity model for steel. From a set of 12 corner-reinforced concrete beam-column subassemblies reported in the experimental reference, two specimens (the LL11 and the LH11) were modeled in order to verify the nonlinear capabilities of the numerical models for reproducing the concentration of shear stresses inside the joints. Since a numerical point of view, these simulations have served to verify the compatibility between different nonlinear formulations, but also for identifying their limitations. In general, all the numerical simulations stopped as soon as a non-convergence condition was reached. From a physical point of view, this non-convergence corresponds to the instant when a set of concrete elements reaches a high level of damage. By comparing experimental curves with numerical results, it can be appreciated that some key-values are very similar (maximal load capacity associated to the lateral displacement), but the shape of their dissipative hysteresis loops are far away from any similitude. The numerical results have allowed corroborating the influence of the stirrups in the resistance of the connection showing their importance. When no stirrups are placed inside the core, the damage is reached almost immediately, even if the longitudinal bars of the column and beams pass through the joint. Conversely, when the number of stirrups is increased inside the core, the principal damage is placed out of the core, exactly in the plane of connectivity between the beam and the core of the connection. Finally, it is necessary to implement bond elements which must redistribute the stresses on the concrete body if any small slip or decohesion occurs between steel bars and concrete, avoiding a false premature degradation of concrete.

References

Alamedinne, F. and Ehsani, M.R. (1991), "High-strength RC connections subjected to inelastic cycling loading", *J. Struct. Eng. - ASCE* , **117**(3), 829-850.

Alcocer, S. (1991), *Comportamiento y diseño de estructuras de concreto reforzado. Uniones de elementos*, CENAPRED/Instituto de Ingeniería-UNAM. (In Spanish).

Chakrabarty, J. (2006), *Theory of plasticity*, Elsevier Butterworth-Heinemann, London UK.

Dominguez, N., Brancherie, D., Davenne, L. and Ibrahimbegovic A. (2005), "Prediction of crack pattern distribution in reinforced concrete by coupling a strong discontinuity model of concrete cracking and a bond-slip of reinforcement model", *Eng. Comput*., **22**(5-6), 558-582.

Ha, G.J. and Cho, C.G. (2008), "Strengthening of reinforced high-strength concrete beam-column joints using advanced reinforcement details", *Mag. Concrete Re*s., **60**(7), 487-497.

Ha, G.J., Cho, C.G., Kang, H.W. and Feo, L. (2012), "Seismic improvement of RC beam-column joints using hexagonal CFRP bars combined with CFRP sheets", *Compos. Struct*., DOI:10.1016/j.compstruct. 2012.08.022.

Ibrahimbegovic, A, Gharzeddine, F. and Chorfi, L. (1998), "Classical plasticity and viscoplasticity models reformulated: theoretical basis and numerical implementation", *Int. J. Numer.Meth. Eng.*, **42**, 499-535.

Ibrahimbegovic, A. (2009), *Non linear solid mechanics*, Springer, London/New York.

Jehel, P., Davenne, L., Ibrahimbegovic, A. and Léger, P. (2010), "Towards robust viscoelastic-plastic-damage material model with different hardenings / softenings capable of representing

salient phenomena in seismic loading applications", *Comput. Concrete*, **7**(4), 365-386.
Karayannis, C.G. and Sirkelis, G.M. (2008), "Strengthening and rehabilitation of RC beam–column joints using carbon-FRP jacketing and epoxy resin injection", *Earthq. Eng. Struct. D.*, **37**(5), 769-790.
Kim, J. and LaFave, J.M. (2007), "Key influence parameters for the joint shear behaviour of reinforced concrete (RC) beam-column connections", *Eng. Struct.*, **29**(10), 2523-2539.
Lowes, L.N. and Moehle J.P. (1995), "Evaluation and retrofit of beam-column T-joints in older reinforced concrete bridge structures", *ACI Struct. J.*, **96**(4), 519-532.
Lowes, L.N. (1999), *Finite element modeling of reinforced concrete beam-column bridge connections*. Ph. D. Thesis, Civil Engineering Graduated Division, University of California, Berkeley, USA.
Lowes, L.N., Mitra, N. and Altoontash, A (2004), *A beam-column joint model for simulating the earthquake response of reinforced concrete frames*, Pacific Earthquake Engineering Research Center, PEER Report 2003/10, University of California, Berkeley, USA.
Ma, S.Y.M., Bertero, V.V. and Popov, E.P. (1976), *Experimental and analytical studies of the hysteretic behavior of reinforced concrete rectangular and T-beams*, Report No. EERC-76-2. Berkeley: EERC, University of California, USA.
Markovic, D. and Ibrahimbegovic, A. (2006), "Complementary energy based FE modeling of coupled elasto-plastic and damage behavior for continuum microestructure computations", *Comput. Method. Appl. M.*, **195**, 5077-5093.
Mazars J. (1986), "A description of micro- and macroscale damage of concrete structures", *Eng. Fract. Mech.*, **25**(5-6), 729-737.
Meinheit, D.F. and Jirsa, J.O. (1977), *The shear strength of reinforced concrete beam-column joints*, CESRL Report No. 77-1. Austin: University of Texas.
Ngo, V.M., Ibrahimbegovic, A. and Brancherie, D. (2014), "Thermomechanics failure of RC composites: computational approach with enhanced beam element", *Coupled Syst. Mech.*, **3**(1), 111-145.
Park, R. and Paulay, T. (1997), *Estructuras de concreto reforzado*. Limusa, México.(In Spanish).
Ragueneau, F., La Borderie, Ch. and Mazars, J. (2000), "Damage model for concrete like materials coupling cracking and friction, contribution towards structural damping: first uniaxial application", *Mech. Cohesive-frictional Mater.*, **5**, 607-625.
Sasmal, S. and Ramanjaneyulu, K. (2012), "Evaluation of strength hierarchy of beam-column joints of existing RC structures under seismic type loading", *J. Earthq. Eng.*, **16**(6), 897-915.
Taylor, R.L. (2005), "FEAP- A finite element analysis program version 7.4. User manual", See: http://www.ce.berkeley.edu/~rlt/feap/ .
Visintin, P., Oehlers, D.J., Wu, C. and Griffith, M.C. (2012), "The reinforcement contribution to the cyclic behaviour of reinforced concrete beam hinges", *Earthq. Eng. Struct. D.*, **41**(12), 1591-1608.
Wang, Y.C. (2012), "Reinforced concrete jacketing for seismic upgrading of RC frames with poor reinforcing details in beam-column joints", *Proceedings of the International Offshore and Polar Engineering Conference*.
Wong, S.H.F. and Kuang, J.S. (2011), "Predicting shear strength of RC exterior beam-column joints by modified rotating-angle softened-truss model", *Comput. Concrete*, **8**(1), 59-70.
Zhou, H. and Zhang, Z. (2012), "Interaction of internal forces of exterior beam-column joints of reinforced concrete frames under seismic action", *Struct. Eng. Mech.*, **44**(2), 197-217.